# Phase Retrieval Implementation for the WFIRST Coronagraph Development Testbed

**David Marx, Brian Kern**
*Jet Propulsion Laboratory, California Institute of Technology, 4800 Oak Grove Drive, Pasadena, CA 91009*
*David.S.Marx@jpl.nasa.gov*

**Abstract:** Phase retrieval is an important tool for the coronagraph testbed at JPL. We present a phase retrieval approach that combines parametric and non-parametric phase estimates using the focused and defocused source images.
**OCIS codes:** (120.5050) Phase Measurement; (100.5070) Phase Retrieval

## 1. Introduction

The Wide-Field Infrared Survey Telescope (WFIRST) is a 2.4m diameter space telescope NASA program. The payload will include two instruments, including a coronagraph instrument (CGI). The CGI will be the first active, high-contrast stellar coronagraph in space intended for imaging, discovery, and spectral characterization of exoplanets and debris discs.

The CGI designs under development use deformable mirrors (DM) to create a point spread function (PSF) with a dark region around the obscured star object. Each DM consists of an array of actuators, and each actuator causes a local displacement to a thin, mirror-coated, glass face sheet. The actuator displacements are designed to create the PSF. Typically, phase retrieval is used to set the DM actuator displacements to their designed pattern, and then the actuators are further modified by an iterative control loop to correct for system non-idealities. To observe an exoplanet near the star object, the contrast in the annular region must be better than 10^8 (10^9 after post processing) relative to the unobstructed image of the star [1,2].

The coronagraph testbed at Jet Propulsion Laboratory is used to test coronagraph design and control algorithms. The optical system (Fig. 1) is maintained in a vacuum tank so that the PSF is stable for long integration times. Phase retrieval is an important tool for the testbed and serves several purposes, in addition to setting initial DM actuator displacements. Other uses include evaluation of systematic wavefront error introduced by system components, and alignment of the DMs and pupil masks. For example, the location of specific DM actuators relative to the Lyot mask can be determined by displacing the actuator, then measuring the location of the phase disturbance in the pupil plane with phase retrieval.

In the next section we further describe the optical train of the testbed and the collection of source and pupil images available as inputs for phase retrieval, as well as one phase retrieval algorithm employed. Section 3 shows example phase retrieval results.

## 2. Phase Retrieval Algorithms Incorporating Defocused Source and Pupil Images

A schematic of the optical layout of the coronagraph testbed is shown in Fig. 1. The final lens, L, can be switched between a lens to form a source image, and a lens of half the focal length to form an image of the pupil. Further, the camera is mounted on a translation stage so that defocused images of the source or the pupil can also be captured. The goal of the phase retrieval is to recover the wavefront phase at the image of the pupil, P'. The telescope pupil, DM1, and the Lyot stop are all conjugate to the pupil image. Measurement of the phase at the pupil image P' provides an estimate of the total systematic phase error, but the measurement requires removal of the Lyot mask, the central stop, and the field mask. The phase retrieval algorithm employed makes use of several defocused source images and pupil images. Because the source images and pupil images are created with different lenses before the camera, an estimate of the difference in phase error between the two lenses also results.

Several phase retrieval algorithms are possible. For example, iteration between the source image and the pupil image is a typical approach. However, since the source image and pupil image are created by different lenses, this phase retrieval approach must allow for relative alignment errors and wavefront errors caused by the lenses. Another approach is to use the source image and a defocused source image in an iterative phase retrieval. Similarly, the pupil image and one or multiple defocused pupil images can be used in an iterative phase retrieval.

The focused and defocused source images, and the focused and defocused pupil images, provide a wide variation of Fresnel numbers, and so phase retrieval can be tailored to emphasize different characteristics. For example, the defocused source image has a Fresnel number approximately 3, and so phase retrieval utilizing the source image and the defocused source image will emphasize low spatial frequency phase characteristics. In contrast, the pupil image

to the defocused pupil image has a Fresnel number on the order of 150. Thus, the diffraction from pupil to defocused pupil is dominated by high spatial frequency phase components, and the low order phase effects are deemphasized.

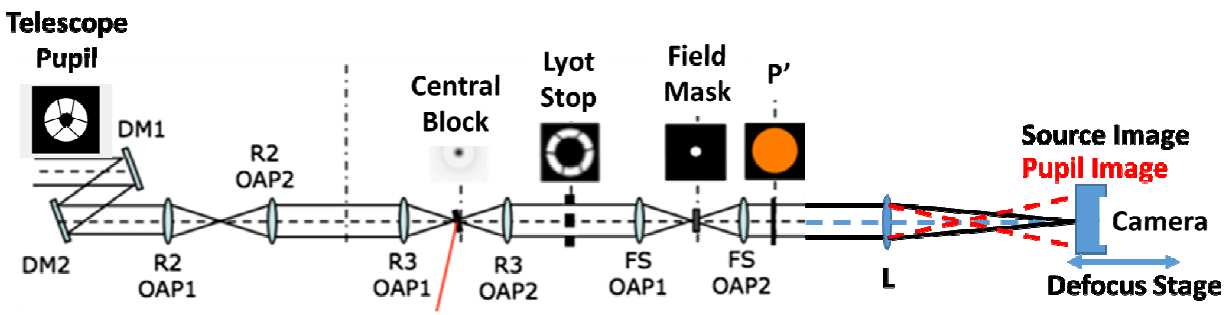


Fig. 1. Coronagraph Instrument layout. The final lens, L, can be switched between a long focal length lens to create an image of the source, or a shorter focal length lens to create an image of the pupil. Normal coronagraph operation is with the source imaging lens, and the pupil imaging lens is used for evaluation and alignment. To measure the system phase error at the pupil image P', the Central Block (Occulter), Lyot Stop, and Field Mask are removed.

For the work presented here, the testbed had flat mirrors in place of the DMs, and the sources of wavefront error were primarily systematic. Therefore, only low spatial frequency phase errors were expected, and we used the source image and defocused source images for phase retrieval. The choice of phase retrieval algorithm used parametric phase retrieval to estimate low order Zernike phase terms, and then used that result as the initial estimate for iterative, non-parametric phase retrieval using defocused source images [3].

The phase variation across the pupil was estimated by the following steps:

1. Translate the source image so that its peak coincides with the calculated psf using the pupil image. Fractional pixel translations are interpolated using two dimensional FFTs.
2. Parametric phase retrieval of the pupil using the scaled pupil image and the focused source image. Non-linear unconstrained optimization where the independent variables are the Zernike terms 4 through 22, and the merit function, MF = $1 - C\,(A_m, A_c)$, where $C\,(A_m, A_c)$ is the statistical correlation of the measured amplitude image and the calculated amplitude image. Only the pixels inside the circular region of radius 5 $\lambda$F# are used in the correlation.
3. Non-parametric phase retrieval of the pupil using the scaled pupil image and multiple de-focused source images. The initial pupil phase is the result of the parametric fitting (step 2). Each iteration included: propagating the pupil to the first defocused source image; imposing the measured amplitude while keeping the calculated phase; propagating back to the pupil; imposing the pupil amplitude; propagating to the next defocused source image; and repeat. Correlation coefficients of the measured and calculated amplitude images were monitored for convergence.

## 3. Results

Results of the parametric and non-parametric phase retrieval calculations are shown in Figs. 2 and 3. In each of these figures, the left image is the measured amplitude (square root of the intensity), the middle image is the calculated amplitude at the end of the phase retrieval method, and the right image is the calculated pupil phase. The result of the parametric phase retrieval shows that the optical system suffers from significant astigmatism, likely a misalignment in the telescope source. The pupil phase resulting from the parametric phase retrieval was used as the initial condition for the iterative non-parametric phase retrieval using the defocused source images. A measure of the success of the phase retrieval algorithm is the correlation coefficient between the measured amplitude and the calculated amplitude. After 100 iterations, the correlation coefficient was 0.95 for both defocused source images. At the time these images were recorded, the DMs were replaced by fixed mirrors, and so only low spatial frequency phase features were expected.

## 4. Conclusions

To achieve the contrast necessary to observe exoplanets, the coronagraph system must be well-characterized, and the wavefront tightly controlled. Phase retrieval is an important tool. The WFIRST coronagraph testbed was designed for flexibility to allow phase retrieval using pupil images, source images, and defocused images of either the pupil or the source. With all of these various images available, many different phase retrieval approaches are possible.

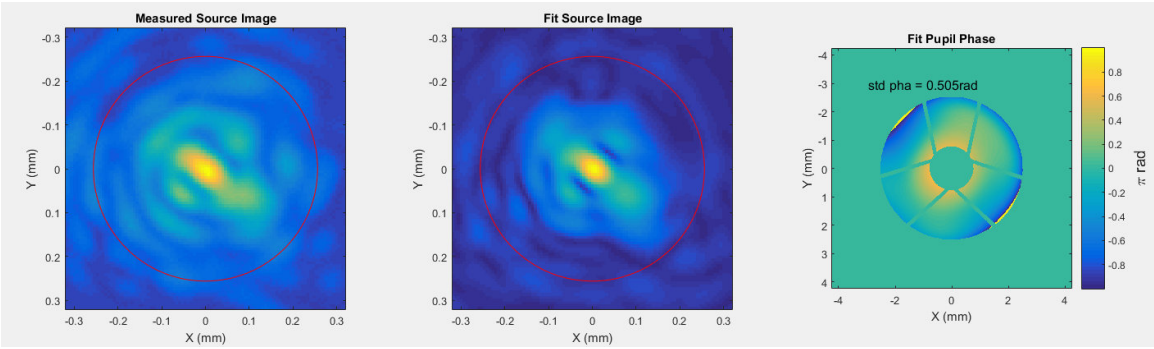


Fig. 2. Measured intensity and estimated phase resulting from the parametric phase retrieval. The left image is the measured amplitude of the focused source image. The center image is the source image amplitude calculated by propagating the pupil with the phase map as shown in the right image. The phase map was constructed by the parametric phase retrieval using the first 22 Zernike terms.

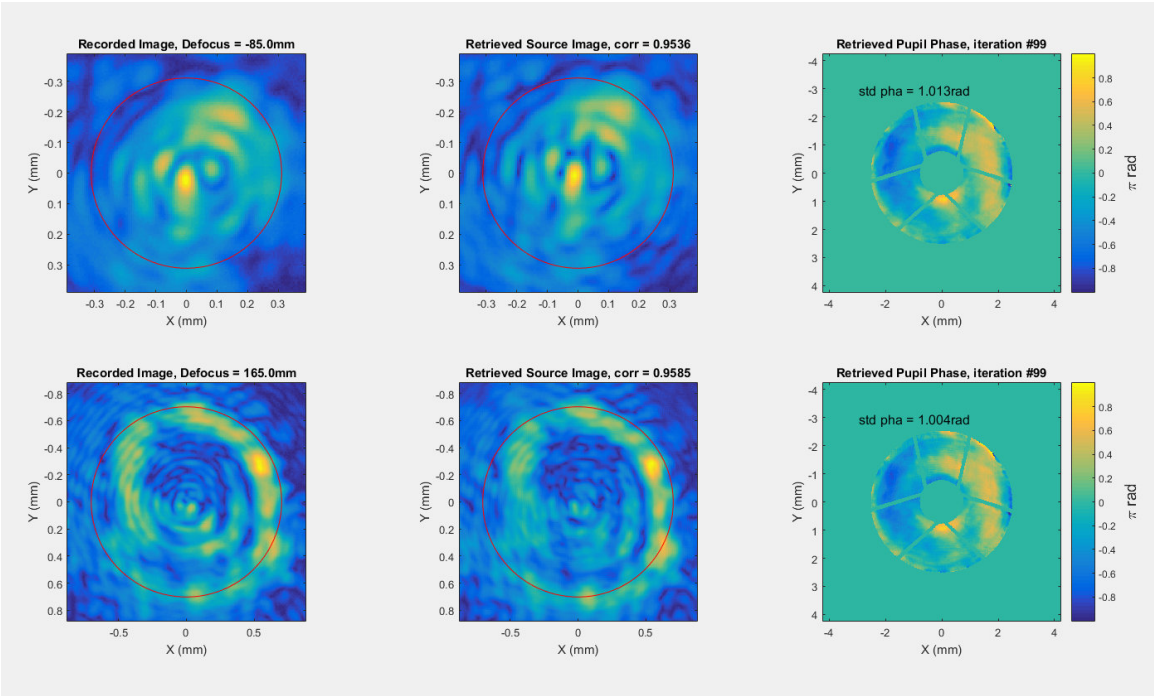


Figure 3. Measured (left column) and calculated (center column) amplitude images for two defocused source images. The right column are retrieved pupil phase. The total pupil phase is the sum of the parametric phase retrieval result and the phase map shown in this figure. The top row is for source images at -85mm defocus, and the bottom row is for source images at +165mm of defocus.

## 5. Acknowledgement

The research was carried out at the Jet Propulsion Laboratory, California Institute of Technology, under a contract with the National Aeronautics and Space Administration.

## 6. References

[1] M. Charley Noecker, Feng Zhao, Rick Demers, John Trauger, Olivier Guyon, and N. Jeremy Kasdin, "Coronagraph Instrument for WFIRST-AFTA," J. Astron. Telesc. Instrum. Syst. Vol. 2, p. 011001-1 (2016).

[2] Amir Give'on, Brian Kern, Stuart Shaklan, Dwight C. Moody, and Laurent Pueyo, "Broadband Wavefront Correction Algorithms for High-contrast Imaging Systems," in SPIE Proceedings Vol. 6691, Astronomical Adaptive Optics Systems and Applications III, (SPIE, 2007).

[2] John E. Krist and Christopher J. Burrows, "Phase-retrieval Analysis of Pre- and Post-repair Hubble Space Telescope Images," Applied Optics, Vol. 34, No. 22, pp. 4951-4964 (1995).